Multiobjective Inverse Parameter Estimation for Modelling Vadose Zone Water Movement

Wöhling, Th.[1] and Vrugt, J. A.[2]

[1] Lincoln Ventures Ltd, Lincoln Environmental Research, Ruakura Research Centre, Hamilton, New Zealand.
Email: woehling@lvlham.lincoln.ac.nz
[2] Center for Nonlinear Studies (CNLS), Los Alamos National Laboratory, Los Alamos, NM 87545, USA

EXTENDED ABSTRACT

Inverse modelling techniques for estimating un-saturated soil hydraulic parameters have become increasingly common in the past two decades. In contrast to single-objective parameter estimation which yields a single set of "best fit" parameters, multiobjective parameter estimation results in a number of Pareto optimal solutions which allow the analysis of the trade-off between different, sometimes conflicting, model objectives.

In this study, modelling tools for identification of Pareto optimal sets of vadose zone water transport parameters are presented utilizing the numerical water and solute transport model HYDRUS-1D. Root-mean-square error (RMSE) values are calculated to measure the fit of the simulated and observed pressure head data at three different depths at a vadose zone of volcanic origin in New Zealand. Gradient based search algorithms fail to reliably find the global optimum in the corresponding objective space exhibiting multiple minima (Figure 1). Consequently, an efficient multiobjective global optimization algorithm is used to solve the multiobjective problem: The Multiobjective Shuffled Complex Evolution Metropolis (MO-SCEM-UA) algorithm which combines a Markov Chain Monte Carlo sampler with the Shuffled Complex Evolutionary (SCE-UA) algorithm and the probabilistic covariance-annealing process of the Shuffled Complex Evolution Metropolis (SCEM-UA) algorithm.

Prior information about the parameters of the Mualem - van Genuchten (1980) soil hydraulic model is included in the model calibration. For that purpose, single-objective "best fit" parameter sets are estimated with the SCE-UA algorithm and used to calculate the multivariate posterior joint probability density function. The initial population of parameter sets in the MOSCEM-UA run is then sampled from this distribution, and the Pareto solutions derived after 20,000 HYDRUS-1D model evaluations. A decision tool developed enables the user to apply different weights to the three objectives, to analyse the trade-off between these objectives when moving along the Pareto fronts, and to quickly obtain the parameter sets for chosen solutions. The compromise solution is derived by equal weighting the individual objectives. This solution matches well with the observations, which is confirmed by an overall RMSE of 0.16 m. This is an acceptable fit in comparison to the single-objective fits of RMSE = 0.09 / 0.09 / 0.11 m for objectives $F_1 - F_3$ respectively.
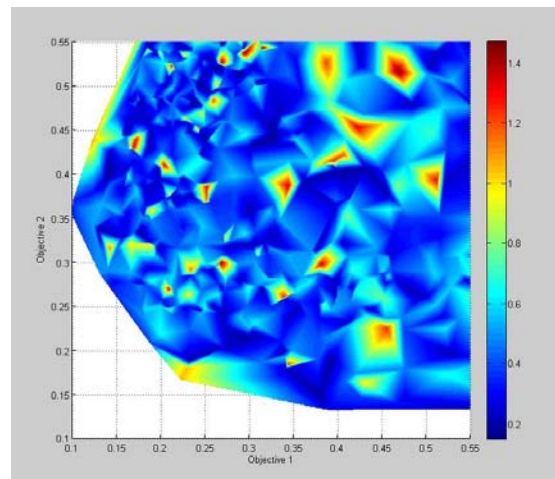
Figure 1. Surface plot of the three-dimensional objective space of the optimization problem to be solved (colour representing values of objective 3). Genetic search algorithms are used to find the global minimum in this search space.

Uncertainty bounds derived by simulation with the Pareto sets are relatively large for both the simulated pressure heads at the three observation locations and the simulated drainage fluxes at the lower model boundary. The analysis further revealed that the large uncertainty may be related to model structural inadequacies neglecting preferential flow paths after prolonged dry periods. Smaller uncertainty bounds could be expected when these processes are incorporated accurately in the model.

1. INTRODUCTION

Information about the hydraulic properties is required when investigating water transport and the fate of solutes in the vadose zone with conceptual or deterministic models. Due to the difficulty of transferring information obtained from small scale samples to larger scale investigations, the estimation of 'effective' parameters by inversion of the modelling problem has become increasingly popular during the past decade (e.g. Inoue et al. 1998, Šimůnek et al. 1998, Si and Kachanoski 2000, Abbasi et al. 2003, Kelleners et al. 2005, Ritter et al. 2005). Various algorithms have been developed to find parameters which yield the best attainable fit between model predictions and observations at the scale of interest. Local search methods seek for systematic improvement of the objective function using an iterative search starting from a single initial point in the parameter space. Such nonlinear gradient-based algorithms (e.g. Levenberg-Marquardt) have found widespread use in the field of vadose zone hydrology but fail to find the global optimum in response surfaces exhibiting multiple optima in the parameter space with both small and large domains of attraction (e.g. Figure 1), discontinuous first derivatives and curved multidimensional ridges. In contrast, robust global optimization methods use multiple concurrent searches from different starting points to reduce the chance of getting stuck in a single basin of attraction. Global optimization methods that have been used for the estimation of the unsaturated soil hydraulic properties include the Annealing Simplex method, Genetic Algorithms, Multilevel grid sampling strategies, and Shuffled Complex methods. In the case of more than a single objective function, the optimization problem is posed in a multiobjective context (e.g. Gupta et al. 1998, Boyle et al. 2000, Deb et al. 2002, Madsen 2003, Vrugt et al. 2003a). By simultaneously employing a number of complementary criteria, and analyzing the trade-offs between the fitting of these criteria, the modeler is able to better understand the limitations of model structures, and gains insights into possible model improvements (Gupta et al. 1998, Tang et al. 2006).

In this study, a multiobjective optimization framework is used for inverse estimation of the hydraulic parameters of a volcanic soil using observed tensiometer data from three different depths at the *Spydia* field site in New Zealand. HYDRUS-1D (Šimůnek et al., 2005) is used for flow modelling, and a root-mean-square error (RMSE) value is defined at each depth to separately measure the ability of the model to simulate the observed tensiometric data at each of these locations. The resulting optimization problem is solved with the Multiobjective Shuffled Complex Evolution Metropolis (MOSCEM-UA: Vrugt et al., 2003b) algorithm. We analyse the trade-off between the three different RMSE objective functions and interpret the HYDRUS-1D model predictions associated with the Pareto optimal parameter sets.

2. METHOD

2.1.   Experimental Data

The *Spydia* site is located in the Tutaeuaua sub-catchment (Landcorp's Waihora Station, E 175.79977, S 38.61423) north of Lake Taupo on a sheep and beef farm under pastoral land use. The vadose zone materials at *Spydia* encompass a young volcanic soil (0 - 1.6 m depth), which belongs to the Oruanui loamy sand series developed on the underlying unwelded Taupo Ignimbrite (TI, 1.6 - approx. 4.4 m) from the 1.8 ka BP Taupo eruption. The deeper layers are influenced by lateral groundwater flow during at least some parts of the year (typically the winter and spring months) and are therefore not included in the calculations. They encompass two older buried soils (Palaeosols, P1 and P2) in approximately 4.5 to 5.8 m depth and Oruanui Ignimbrite (OI) material below.

Table 1: Average textural data for the vadose zone materials as derived from laboratory analysis. The gravel fraction includes all particles >0.002 m. BD denotes the dry bulk density

Sampling depth [m]	Clay [%]	Silt [%]	Sand [%]	Gravel [%]	BD [Mg m^{-3}]
0.05 - 0.10	6	41	51	2	0.75
0.10 - 0.15	5	32	58	5	0.78
0.60 - 0.65	3	23	54	20	0.8
1.80 - 1.85	3	25	40	32	0.81
3.50 - 3.55	3	23	37	37	0.85
3.72 - 4.32[*]	6	41	51	2	0.92

[*] varying sampling depth due to varying layer boundaries

Undistributed soil cores were taken from the vadose zone materials for laboratory analysis of the textural data (shown for relevant depths in Table 1), the total porosity, water retention data, the saturated hydraulic conductivity K_s, and the hydraulic conductivity at -0.4 kPa, $K_{-0.4}$. The total porosity varied between 0.61- 0.68 m^{3}m^{-3} for the materials between land surface and 4.32 m depth and significantly higher (0.70 – 0.74 m^{3}m^{-3}) for the underlying Palaeosols. Median K_s –values ranged from 8E-7 to 1E-5 ms^{-1} with the largest values at the top soil and the smallest at the OI. $K_{-0.4}$ was about 0.1 to 0.2 orders of magnitude smaller than K_s at the cores from the upper soil (0.0 - 0.6 m)

and up to two orders of magnitude smaller at the upper TI materials (1.8 m and 3.5 m depths) and in the Palaeosols. The details of the analysis are reported in Wöhling et al. (2007) and therefore not repeated here.

Tensiometer probes (type UMS T4e, Germany) were installed outward from a central caisson with 2.3 m diameter at five depths (0.4, 1.0, 2.6, 4.2, and 5.1 m - with three replicates at each depth). The tensiometric pressure heads were continuously recorded since March 2006 at 15 min time intervals using a compact FieldPoint controller (cFP2010, National Instruments) programmed for daily remote data transfer.

2.2.   Model Setup

The HYDRUS-1D model (Šimůnek et al. 2005) is used for the simulation of water flow in variably saturated porous media. It utilizes the Galerkin finite element method based on a mass conservative iterative scheme. The model solves the one-dimensional Richards equation:

$$\frac{\partial \theta}{\partial t} = \frac{\partial}{\partial z} K \left(\frac{\partial h}{\partial z} + 1 \right) - S \qquad [1]$$

where θ is the volumetric water content [$L^3\,L^{-3}$], t represents time [T], z is the vertical coordinate (positive upward) [L], h denotes the pressure head [L], K is the unsaturated hydraulic conductivity function [LT^{-1}], and S is a sink term representing processes such as plant water uptake [$L^3\,L^{-3}\,T^{-1}$]. The soil hydraulic properties are described by the Mualem - van Genuchten Model (MVG, van Genuchten 1980):

$$S_e = \frac{\theta - \theta_r}{\theta_s - \theta_r} = \begin{cases} \theta_r + \dfrac{1}{\left[1 + |\alpha h|^n\right]^m} & h < h_s \\ 1 & h \geq h_s \end{cases} \qquad [2]$$

$$K(S_e) = K_s S_e^l \left[1 - \left(1 - S_e^{1/m}\right)^m\right]^2 \qquad [3]$$

where S_e is the effective water content, θ_r and θ_s denote the residual and saturated water content respectively [$L^3\,L^{-3}$], α [L^{-1}] and n [-] are parameters that define the shape of the water retention function, K_s represents the saturated hydraulic conductivity [LT^{-1}], l is the pore-connectivity parameter, and h_s is the air entry value. In this study $m = 1 - 1/n$ and $n > 1$ is assumed.

The initial and boundary conditions used to solve Eq. [1] are:

$$h(z,t) = h_i(z) \quad \text{at } t = 0 \qquad [4]$$

$$h(z,t) = h_L(t) \quad \text{at } z = L \qquad [5]$$

and

$$-K \left(\frac{\partial h}{\partial z} + 1 \right) = q_0(t) - \frac{\partial h}{\partial t} \qquad \text{at } z = 0, \text{ for } h_A \leq h \leq h_s$$
$$h(0,t) = h_A \qquad \qquad \text{for } h < h_A$$
$$h(0,t) = h_s \qquad \qquad \text{for } h > h_s \qquad [6]$$

where $h_i(z)$ is the initial pressure head derived from linear interpolation of observed tensions at the 0.4, 1.0, 2.6, and 4.2 m depths, $h_L(t)$ is the prescribed (observed) pressure head at the bottom boundary $L = -4.2$ m (depth of the model is 4.2 m), $q_0(t)$ is net infiltration rate (i.e. precipitation minus evaporation) and h_A and h_s are minimum and maximum pressure head allowed at the soil surface. Eq. [6] describes the atmospheric boundary condition at the soil-air interface (Šimůnek et al. 2005). Because this study deals with relatively coarse textured materials with high infiltration capacity, the infiltration-excess overland flow is neglected and the limits $h_A = -200$ m and $h_s = -0.02$ m are used.

The HYDRUS-1D model was set up for three horizons corresponding to the first three layers of the more recent materials (0 - 0.69 m depths), the disturbed Taupo Ignimbrite (0.69 - 1.6 m) and the in-situ Taupo Ignimbrite (1.6 - 4.2 m), respectively. A uniform spatial discretization of $\Delta x = 0.02$ m (211 nodes) was used for the HYDRUS-1D calculation grid.

Simulations were done for the period of 282 days (April 11, 2006 to January 18, 2007). The initial pressure heads at April 11, 2006 were -0.41, -1.38, -1.18 and -0.85 m at the 0.4, 1.0, 2.6, and 4.2 m depths, respectively. Daily values of potential evaporation were calculated by the Penman-Monteith equation (Allen et al. 1998) using data from the nearby Waihora meteorological station. Precipitation was recorded on site using a 0.2 mm bucket gauge. Values were summed to hourly intervals for use in the calculations. The plant water uptake, S in Eq. [1], is simulated by the Feddes model (1978) using HYDRUS-1D default parameters for grass and an average (measured) depth of the active root zone of 0.35 m.

Three criteria are used to measure the difference between observed and simulated tensiometric data: the root-mean-square error RMSE, the coefficient of determination R^2, and the coefficient of efficiency by Nash-Sutcliffe C_e (ASCE 1993).

2.3.   Inverse Modelling

The proposed method aims to find MVG model parameters values that provide the best attainable fit between model predictions and corresponding observations. A multiobjective framework with

three different criteria is considered,

$$\min F(u) = \begin{bmatrix} F_1(u) \\ F_2(u) \\ F_3(u) \end{bmatrix} \qquad [8]$$

where F_1 - F_3 are the RMSE of the fit between the simulated and observed pressure heads at 0.4, 1.0, and 2.6 m depths, and u is a vector of k model parameters to be optimized. The residual water content θ_r is typically least sensitive to the calibration data (Inoue et al. 1998, Šimůnek et al. 1998, Kelleners et al. 2005) and therefore set to zero. Five MVG model parameters, namely θ_s, K_s, α, n, and l, are estimated in each of the three layers resulting in a 15-dimensional optimization problem ($k = 15$).

To solve the multiobjective framework expressed in Eq. [8], the Multiobjective Shuffled Complex Evolution Metropolis (MOSCEM-UA) algorithm (Vrugt et al. 2003a) was used. The algorithm combines a Markov Chain Monte Carlo sampler with the Shuffled Complex Evolutionary (SCE-UA) algorithm (Duan et al. 1992) and the probabilistic covariance-annealing process of the Shuffled Complex Evolution Metropolis (SCEM-UA) algorithm (Vrugt et al. 2003b). MOSCEM-UA uses the concept of Pareto dominance to evolve the initial population of points toward a set of solutions stemming from a stable distribution. For more details on the algorithm refer to Vrugt et al. (2003a). The MOSCEM-UA performance is sensitive to three algorithmic parameters: the population size s, the maximum (total) number of function evaluations $ndraw$, and the number of complexes/sequences q. In this study, $s = 200$, $ndraw = 20,000$, and $q = 4$ is used.

Multiobjective optimization does not result in a single unique set of parameters but consists of a Pareto set of solutions (e.g. Gupta et al. 1998, Madsen 2003). Pareto optimal parameter sets represent trade-offs among the different objectives having the property that moving from one solution to another results in the improvement of one objective while causing deterioration in one or more others (Vrugt et al. 2003a). Ideally, the multiobjective optimization algorithm should find all Pareto optimal solutions. The trade-off between the different objectives is analysed by mapping the approximated Pareto set from the parameter (decision) space to the objective space.

Prior information about the location of the Pareto distribution in the parameter space is derived from the single criterion solutions (i.e. the Pareto extremes) of the individual objectives and then used for sampling the initial population of parameter sets to be iteratively improved with the optimization algorithm. This methodology was developed by Vrugt et al. (2003a) and summarized below. First, the best attainable parameter values ($u_{i,opt}$) were located for each of the objectives F_i individually using the SCE-UA global optimization algorithm (Duan et al., 1992). Secondly, the multivariate posterior joint probability density function $p(u_i \mid \mathbf{y})$ was approximated at each of the solutions i using a traditional first-order approximation (Box and Tiao 1973):

$$p_i(u \mid \mathbf{y}) \propto \exp\left[-\frac{1}{2\sigma^2} (u - u_{i,opt})^T \mathbf{J}^T \mathbf{J} (u - u_{i,opt}) \right]$$
$$[9]$$

where σ is the RMSE of the fit of the final solution, and $\mathbf{J}$ is the Jacobian or sensitivity matrix evaluated numerically at $u_{i,opt}$. Finally, the initial population for the MOSCEM-UA algorithm was generated by sampling s / M points from the density function specified in Eq. [9] for each individual objective. For more details on the sampling procedure refer to Vrugt and Bouten (2002) and Vrugt et al. (2003a).

3. RESULTS AND DISCUSSION

The results of the study are presented in Figures 2, 3 and 4 and discussed below. Figures 2a-c show the MOSCEM-UA Pareto optimal solutions in the F_1 - F_2, F_1 - F_2, and F_1 - F_3 planes of the three-dimensional objective space. Rank 1 Pareto points (cf. Vrugt et al., 2003a for Pareto ranks) of the last 2,000 HYDRUS-1D evaluations are indicated with black circles in each of the panels. It appears that considerable trade-off exists between objectives F_1 and F_2 (Figure 2a). On the contrary, the other two-dimensional plots exhibit a rather rectangular trade-off pattern demonstrating that the HYDRUS-1D model is able to minimize these objectives simultaneously using a single combination the hydraulic parameters. The density of Pareto points along the F_3 - axis (y-axis in Figures 2b and 2c) is significantly smaller than the density along the other axes, demonstrating a preference of the MOSCEM-UA method to sample along the first two objectives. The reason for the curved F_1 - F_2 Pareto front is most likely found in the model structure. It is assumed that water transport occurs solely through the soil matrix and the presence and dynamics of preferential flow paths is neglected. These quick flow paths develop at least temporally close to the soil surface and hence may have an impact on measured pressure heads at the 0.4 m depth (measured in objective F_1). Other potential model structural inadequacies include the zonation of the strongly stratified vadose zone at the ex-

perimental site in only three different layers and the assumption of uniform water uptake in the root zone.
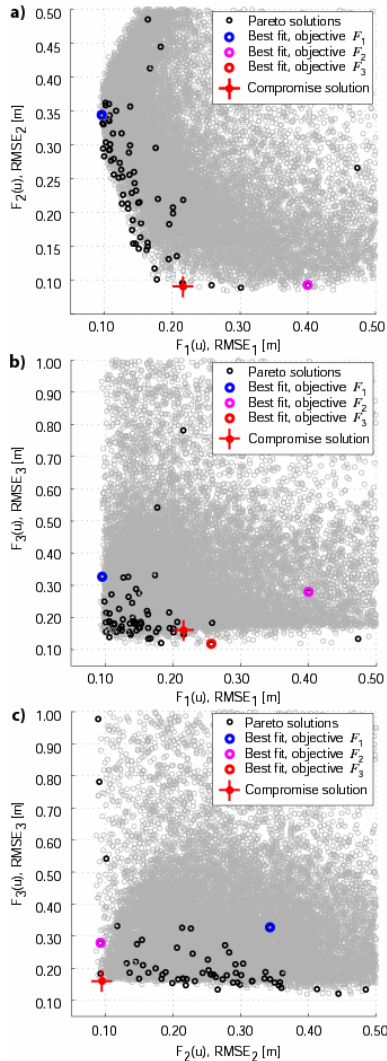

Figure 2: Pareto optimal solutions (solid circles) of the three-dimensional Pareto trade-off space. Compromise solution and single-objective best-fit solutions are also shown (best-fit of objective F_3 with $RMSE_3 = 0.58$ m is beyond axes limit)

To further analyse the results, four different Pareto points are isolated from the analyses which are most informative about the efficiency of the optimization algorithm. The first three Pareto points are the best solutions with respect to each of the individual objectives (Pareto extremes $RMSE_1$, $RMSE_2$, $RMSE_3$). The fourth point is a compromise solution defined by the minimum average RMSE of the three objectives. The Pareto extremes found by the MOSCEM-UA algorithm have a performance of $RMSE_1 = 0.09$ m, $RMSE_2 = 0.08$ m and $RMSE_3 = 0.12$ m ($R_1^2 = 0.91$, $R_2^2 = 0.92$, R_3^2

$= 0.64$ and $C_{e,1} = 0.91$, $C_{e,2} = 0.92$, $C_{e,3} = 0.63$). The compromise solution has a slightly higher RMSE value of 0.16 m. The corresponding parameter values of this solution are listed in Table 2.
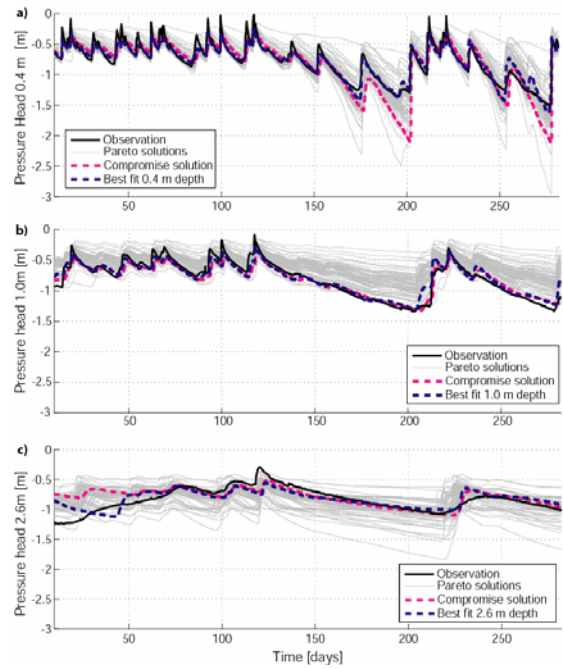

Figure 3: Observed and simulated pressure head using Pareto optimal parameter sets. The compromise solution parameter set and the best fit parameter sets for the objectives F_1, F_2, F_3 (Pareto extremes) also indicated.

Figures 3a-c depict time series plots of HYDRUS-1D model predictions of the pressure head at 0.4, 1.0 and 2.6 m depths. Each grey line going from left to right across the time series plot denotes the prediction of a single Pareto solution, whereas the solid black line represents the observed values. Notice, that the predictions generally cover the tensiometric observations and that the best solutions for the individual depths (dashed blue lines) match well with the observations. The fit is similarly good for the compromise solution parameter set (dashed magenta lines), as previously reported RMSE values are within close range of the optimized values for each individual objective. In fact, the simulation with the compromise solution results in a somewhat lower fit to each individual objective (RMSE = 0.15 / 0.12 / 0.19 m, $R^2 = 0.80$ / 0.87 / 0.19, and $C_e = 0.75$ / 0.81 / 0.01). At the 0.4 m depth, it results in increasing deviations of simulated tensions from observed tensions after prolonged dry periods (Figure 3a). This might be the result of developing preferential flow paths near the soil surface. Both the single-objective solution and the compromise solution at the 0.4 m and 2.6 m depths are found in the centre of the

Pareto prediction intervals (Figure 3a and c), whereas the predictions for the 1.0 m depth are found at the lower end of the Pareto prediction intervals (Figure 3b).
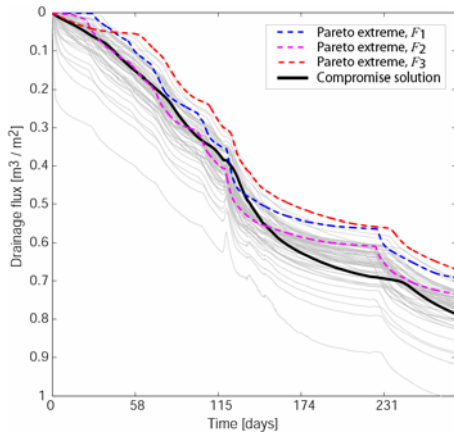

Figure 4: Simulated cumulative flux across the lower model boundary using Pareto optimal parameter sets including the compromise solution and the best fits to the individual objectives (Pareto extremes).

Figure 4 shows the cumulative water flux across the lower model boundary at 4.2 m depth for all Pareto solutions (grey lines). The compromise solution (solid black line) is well bracketed by the Pareto solutions. However, the prediction boundaries are relatively large. Interestingly, the best fit solution with respect to the lowest vadose zone layer (2.6m depth, F_3) results in the lowest cumulative flux. Given equal uncertainty associated with all pressure head data, the results further indicate that smaller prediction bounds for simulated pressure head and flux can be expected when the model structure is improved adequately.

Table 2: Optimized parameter sets for the compromise solution (smallest overall RMSE)

Parameter	Layer 1	Layer 2	Layer 3
θ_s [m^3 m^{-3}]	0.64	0.46	0.54
α [m^{-1}]	7.30	15.55	9.42
n [-]	2.19	1.74	2.04
K_s [m s^{-1}]	8.06E-5	4.96E-4	9.66E-4
l [-]	0.54	0.52	0.52

A software tool was developed which helps the analysis of the results and the choice of parameter sets for predictive simulations. The user assigns weights to each of the individual objectives accordingly to his/her subjective preferences and the program computes the best-fit Pareto solution corresponding to that choice. The fit of the simulations to the observations can be analysed both nu-

merically and visually for the three objectives (Figure 5). Corresponding parameter values are also shown.
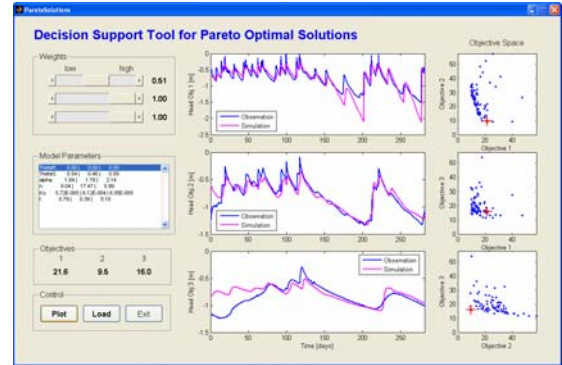

Figure 5: Software tool for quick analysis of the Pareto solutions.

4. CONCLUSIONS

A methodology for multiobjective estimation of vadose zone model parameters with the MO-SCEM-UA algorithm was presented and simulation results using the Pareto parameter sets analysed. Simulations of pressure head at the observation locations using either the Pareto extremes for the various objectives or the parameter combination of the compromise solution resulted in a good match to the measured pressure head values. Perhaps more importantly, the Pareto prediction bounds generally encapsulated the observed data, but were quite large. Access to the entire Pareto distribution is supported by a software tool, which increases insight into model structural inadequacies, and helps select a single value for the various hydraulic parameters that provide acceptable trade-off between the various objectives.

5. REFERENCES

Abbasi, F., D. Jacques, J. Šimůnek, J. Feyen, and M.Th. van Genuchten (2003), Inverse estimation of soil hydraulic and solute transport parameters from transient field experiments: Heterogeneous soil, *Transactions of the ASAE*, 46(4):1097-1111.

Allen, R.G., L.S. Pereira, D. Raes, and M. Smith (1998), Crop evapotranspiration. *FAO Irrigation and Drainage Paper No. 56*, Rome (Italy).

ASCE. 1993. Task committee on definition of watershed models of the watershed management committee: Criteria for evaluation of watershed models. *J. Irrig. Drain. Div.*, 119(3):429-442.

Box, G.E.P. and G.C. Tiao (1973), Bayesian inference in statistical analysis. Addison-Wesley series in behavioral science. Addison-Weslay Publishers Co., Reading, Mass. 588p.

Boyle, D.P., H.V. Gupta and S. Sorooshian (2000), Toward improved calibration of hydrological models: Combining the strengths of manual and automatic methods. *Water Resour. Res.*, 36:3663-3674.

Celia, M.A., E.T. Bouloutas, and R.L. Zarba (1990), A general mass-conservative numerical solution for the unsaturated flow equation. *Water Resour. Res.*, 26(7):1483-1496.

Deb, K., A. Pratap, S. Agarwal and T. Meyarivan (2002), A fast and elitist multi-objective genetic algorithm: NSGA-II. In *IEEE Trans. Evol. Comp.*, 6, 182-197.

Duan, Q., S. Sorooshian and V.K. Gupta (1992), Effective and efficient global optimization for conceptual rainfall-runoff models. *Water Resour. Res.*, 28:1015-1031.

Feddes, R.A., P. Kowalik and H. Zaradny (1978), Simulation of field water use and crop yield. PUDOC, Wageningen, Netherlands. ISBN 90-220-0676-X.

van Genuchten, M.Th (1980) A closed-form equation for predicting the hydraulic conductivity of unsaturated soils. *Soil Sci. Soc. Am. J.*, 44(5):892-898.

Gupta, H.V., S. Sorooshian and P.O. Yapo (1998), Toward improved calibration of hydrologic models: Multiple and noncommensurable measures of information. *Water Resour. Res.*, 34(4):751-764.

Inoue, M., J. Šimůnek, J.W. Hopmans and V. Clausnitzer (1998), In situ estimation of soil hydraulic functions using a multistep soil-water extraction technique. *Water Resour. Res.*, 34(5):1035-1050.

Kelleners, T.J., R.W.O. Soppe, J.E. Ayars, J. Šimůnek and T.H. Skaggs (2005), Inverse analysis of upward water flow in a groundwater table lysimeter. *Vadose Zone J.*, 4:558-572.

Madsen, H. (2003), Parameter estimation in distributed hydrological catchment modelling using automatic calibration with multiple objectives. *Adv. Wat. Resour.*, 26:205-216.

Ritter, A., R. Munoz-Carpena, C.M. Regalado, M. Javaux, and M. Vanclooster (2005), Using TDR and inverse modeling to characterize solute transport in a layered agricultural volcanic soil. *Vadose Zone J.*, 4:300-309.

Si, B.C. and R.G. Kachanoski (2000), Estimating soil hydraulic properties during constant flux infiltration: Inverse procedures. *Soil Sci. Soc. Am. J.*, 64(2):439-449.

Šimůnek, J., M.Th. van Genuchten, and M. Šejna (2005), The HYDRUS-ID Software Package for Simulating the One-Dimensional Movement of Water, Heat, and Multiple Solutes in Variably-Saturated Media. Version 3.0. Department of Environmental Sciences, University of California Riverside, Riverside, CA, 92521, USA.

Šimůnek, J., O. Wendroth, and M.Th. van Genuchten (1998), Parameter estimation analysis of the evaporation method for determining soil hydraulic properties. *Soil Sci. Soc. Am. J.*, 62:894-905.

Tang, Y., P. Reed, and T. Wagener (2006), How effective and efficient are multiobjective evolutionary algorithms at hydrologic model calibration? *Hydrol. Earth Syst. Sci.*, 10:289-307.

Vrugt, J.A. and W. Bouten (2002), Validity of first-order approximations to describe parameter uncertainty in soil hydrologic models. *Soil Sci. Am. J.*, 66:1740-1751.

Vrugt, J.A., H.V. Gupta, L.A. Bastidas, W. Bouten, and S. Sorooshian. 2003a. Effective and efficient algorithm for multiobjective optimization of hydrologic models. Water Resources Research, 39(5):1-19.

Vrugt, J.A., H.V. Gupta, W. Bouten, and S. Sorooshian. 2003b. A Shuffled Complex Evolution Metropolis algorithm for optimization and uncertainty assessment of hydrologic model parameters. Water Resources Research, 39(8).

Wöhling, Th., J.A. Vrugt, G.F. Barkle (2007), Comparison of three multiobjective algorithms for inverse modelling of vadose zone hydraulic properties, *Soil Sci. Soc. Am. J.* (in press)